Variation of heat radiative fluxes and cooling rates at varying amounts of an absorber

L.I. Nesmelova, O.B. Rodimova, and S.D. Tvorogov

Institute of Atmospheric Optics,
Siberian Branch of the Russian Academy of Sciences, Tomsk

Received July 16, 1999

Heat radiative fluxes and cooling rates are calculated with the use of approximation formulas for transmission functions. The altitude distributions are obtained for contributions from different spectral regions to the radiative fluxes and cooling rates. The behavior of these distributions is studied at varying amounts of such absorbers as water vapor and carbon dioxide in the atmosphere.

1. Introduction

The influence of atmospheric admixtures on the altitude behavior of atmospheric temperature has been studied, as a rule, within the framework of one-dimensional radiative–convective models. By now a large number of papers have been published in which radiative fluxes and cooling rates were found using the line-by-line method for different standard models of the atmosphere, as well as for the case of varying concentration of some minor atmospheric constituents. Among these papers we would like to note Ref. 1, in which the radiative parameters were calculated with due attention to the accuracy of calculation. References 2 and 3 present the tables of altitude behavior of the radiative fluxes and rates for some model atmospheres recommended by the ICRCCM in order to compare the results of radiative computer codes.

References 4 and 5 present detailed calculations of the cooling rate profiles and spectral distribution for the longwave spectral region with the allowance for water vapor, carbon dioxide, ozone, methane, nitrogen oxides, and hydrocarbons within the tropical atmosphere and midlatitude summer and winter. It is shown that the contribution of water vapor strongly depends on wavelength. For perturbations in the lower troposphere, the maximum response is observed in the 8–12-μm transmission window, whereas perturbations in the upper troposphere result in the maximum response in the region of rotational–vibrational bands (< 8 μm) and in the purely rotational band (> 12 μm).

In Ref. 6 particular attention is paid to how the spread in determination of model concentration and temperatures influences the calculated cooling rates. The influence of variations in the atmospheric composition on the outgoing radiation F and the greenhouse effect $G = E - F$ (E is the surface emission) was studied in Ref. 7. The latter paper again studies the influence of doubling of the CO_2 content on these parameters, as well as the contribution due to vertical perturbations in the water vapor content for the atmospheres of arctic winter and tropical summer. In calculations of the outgoing radiation, the proportional increase in CO_2 and H_2O concentrations over the whole depth of the atmosphere, as well as an individual increase in H_2O concentration in one of the three altitude ranges: surface – 800, 800 – 500, and 500 mbar – upper boundary of the atmosphere, were taken as perturbations. The pattern of altitude–spectral distribution of the difference in cooling rates was obtained for a proportional increase in CO_2 and H_2O concentrations for the atmospheres of the arctic winter and tropical summer.

The calculations of radiative fluxes by the line-by-line method as in the above-mentioned references are rather cumbersome and computationally expensive. Therefore, the problems solved therein are reduced, as a rule, to single calculation (for example, the cooling rate profile is calculated at given concentrations of substances studied, within a given model of the atmosphere). To reveal qualitative peculiarities in the behavior of concentrations, such as drastic increase or decrease in temperature, single calculation is obviously insufficient.

We would like to systematize, in a certain way, the approach to analysis of the influence of varying minor gaseous constituents on radiative fluxes, cooling rates, and finally on the altitude behavior of the atmospheric temperature. The first problem in this context is to find the altitude–spectral distribution of variations in radiative fluxes and cooling rates at varying gas composition, as well as to localize the variations in the gas composition and regions (both spectral and altitude) where the variations are maximum. The next problem is to determine the standard altitude behavior of temperature within the framework of a simple radiative model and to analyze it qualitatively on the assumption of critical variations of the gas composition. Finally, we plan to perform line-by-line calculations for the ranges of parameters determined in a simple radiative model. The subject of the discussion in this paper is the first problem.

0235-6880/99/09 764-07 $02.00

Note that because now we consider a simple model and perform only qualitative analysis, there is no need in very high accuracy of calculations. However, it is desirable that the model provides for sufficiently fast calculations thus allowing us to study a wide variety of situations. Therefore, at this stage we prefer to use simpler method for calculation of the transmission function than the line-by-line method. McClatchey et al.[8] have derived formulas for the transmission functions of water vapor, carbon dioxide, and ozone that approximate the results of line-by-line calculations in the region 0–3000 cm^{-1} divided into ten characteristic spectral regions. These formulas have been used in Ref. 8 to study the behavior of cooling rates for individual spectral regions and different models of the atmosphere, and the results obtained in such a way agreed well with more accurate calculations. Using these formulas, we have calculated the longwave radiative fluxes and cooling rates. Thus we have obtained the altitude distributions of the contributions from different spectral regions to the radiative fluxes and cooling rates. On the one hand, these distributions themselves are interesting for us. They help us to answer the question on whether the system response to variations in concentrations of gaseous constituents is selective in altitude and spectral region or not. On the other hand, as was already mentioned, the obtained distributions can be then used for selection of the variability ranges of the parameters in investigation of temperature variations according to our model.

2. Calculated results

To calculate radiative fluxes and cooling rates with a sufficient accuracy, one has to overcome several difficulties. The most serious among them concerns the integration over altitude (pressure). As was already mentioned, our purpose is to draw qualitative conclusions on the spectral and altitude behavior of radiative fluxes and cooling rates. This requires numerous calculations to be performed. So we restrict ourselves to the minimal accuracy at which the qualitative peculiarities in the altitude behavior of the above-mentioned parameters may yet be discerned. We select the standard 33-layer model of the atmosphere[9] and the values of the Planck function calculated at the center of a layer to characterize this layer. All calculations presented in this paper were carried out for the midlatitude summer model of the atmosphere.

Figure 1 shows the calculated results on the cooling rate. The comparison with the line-by-line calculations[11] shows that, on the whole, the character of altitude dependence and its change due to the allowance made for the continuum qualitatively coincide. The discrepancy near the surface is a consequence of our choice of the altitude grid. The discrepancies near the maximum cooling rate at high altitudes are caused by different forms of the continuum used in Ref. 11 and in derivation of the formulas for the transmission functions in Ref. 8.

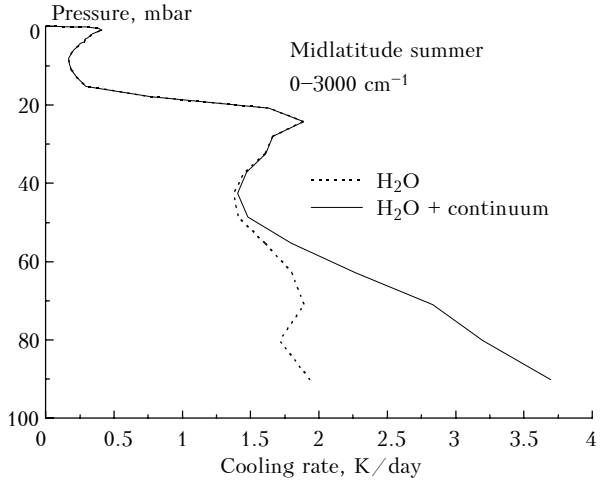

Fig. 1. Cooling rates due to water vapor for the atmosphere of midlatitude summer calculated with the neglect of continuum.

Keeping in mind the above restrictions, we will try to reveal how variations in the concentration of water vapor and carbon dioxide influence the spectral and altitude distributions of cooling rates and radiative fluxes. Such distributions can be presented in the form of 3D images, as shown in Fig. 2 for the cooling rate.

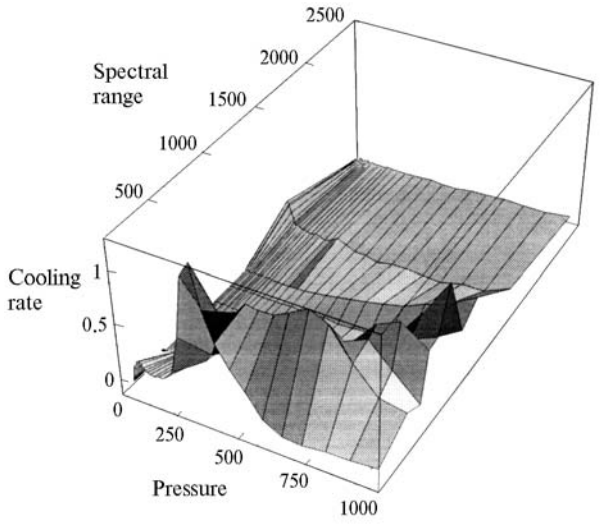

Fig. 2. Spectral–altitude distribution of the cooling rates caused by the standard altitude distribution of the water vapor concentration for the atmosphere of midlatitude summer.

In recent papers (see Refs. 4, 5, and 7) devoted to this subject, such images have been given in 2D presentation with variations of the third coordinate marked by different colors. As in Ref. 8, we accept the following separation of the spectrum into regions: 0–340, 340–540, 540–620, 620–720, 720–800, 800–980, 980–1100, 1100–1380, 1380–1900, and 1900–3000 cm^{-1}.

In the plots each region is characterized by its central frequency. To characterize variations, we use the ordinary and relative differences of the rates and fluxes.

2.1. Continuum absorption

The continuum absorption by water vapor, being relatively small itself, plays a significant part in the formation of outgoing Earth's radiation. Let us consider how the allowance for the water vapor absorption continuum changes the above-mentioned distributions within the framework of our calculations. Figure 3 shows the spectral–altitude distributions of the ordinary and relative differences of the cooling rates between the cases of H_2O and (H_2O+continuum). As in Ref. 8, we take the continuum absorption into account in the 540–1380-cm^{-1} region.

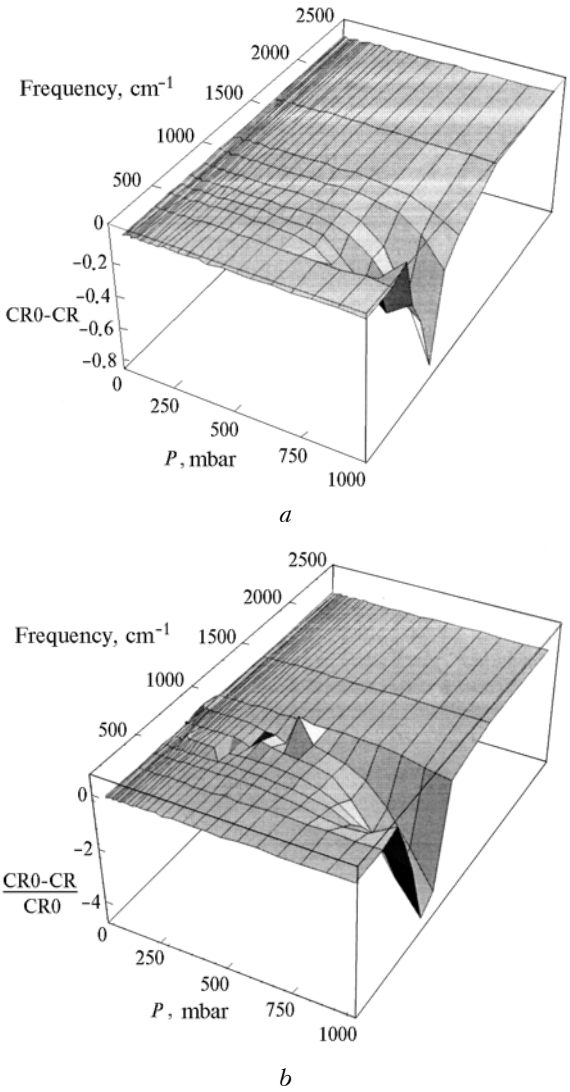

Fig. 3. The ordinary (*a*) and relative (*b*) differences of cooling rates (CR) vs. pressure and spectral region.

It is just this region where we observe maximum variations of the cooling rates that generally tend to the surface and are negative, what means the growth of the cooling rate with allowance for the continuum. However, one can see the regions of nonmonotonic variations, which are more evident in the figure showing the relative differences. More detailed consideration allows us to separate out the spectral region of 540–620 cm^{-1} where the allowance for the continuum introduces the maximum change in the cooling rate at the pressure about 800 mbar rather than on the ground (Fig. 4). Note also that the largest values of the relative differences in the cooling rates fall into other spectral regions.

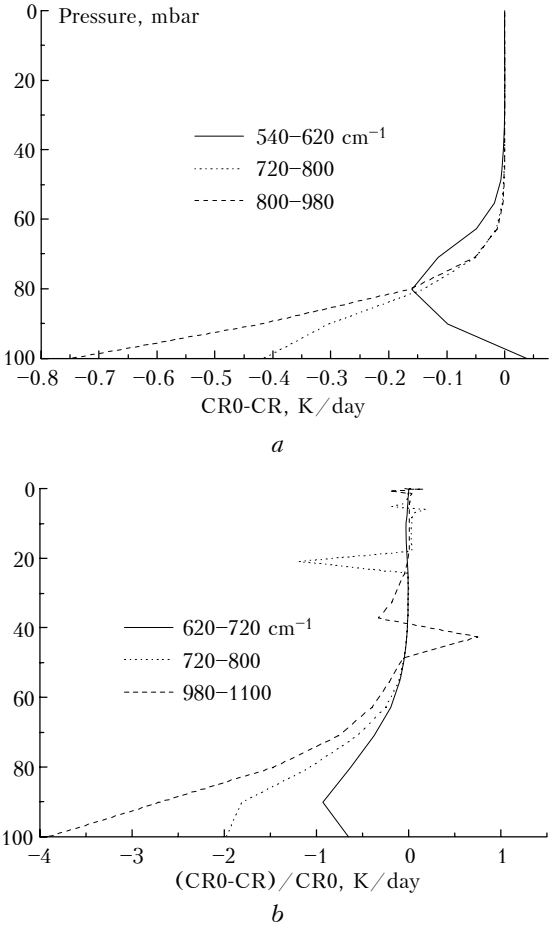

Fig. 4. Ordinary (*a*) and relative (*b*) differences in the cooling rates corresponding to the cases of (H_2O) and (H_2O + continuum) vs. pressure for the spectral regions, where they have the largest values.

Next consider the influence of the change in the temperature dependence of the continuum absorption (its constant varying from 1500 to 4000, instead of 1800) on the cooling rate. Figure 5 illustrates the changes in the ordinary and relative differences of the cooling rates. The largest changes in the cooling rates are concentrated in the altitude range ~900–600 mbar with the maxima somewhat shifted in altitude

depending on the spectral region (Fig. 5*a*). The localized response is observed for the relative differences. Thus, the change in the temperature dependence exerts the largest effect of the relative differences in the cooling rates in the 980–1100-cm^{-1} spectral region at a pressure about 400 mbar (Fig. 5*b*).

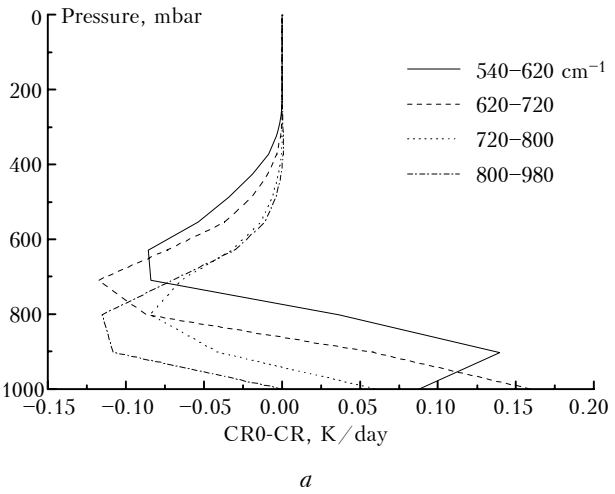

Fig. 5. Ordinary (*a*) and relative (*b*) differences in the cooling rates corresponding to the cases of (H_2O + continuum) and (H_2O + continuum (1800→4000)) vs. pressure for the spectral regions, where they have largest values.

Taking into account of the continuum results in a smooth change of the radiative fluxes. The total flux varies most widely near the surface, and its largest variation (increase by 15–20 W/m^2) falls in the region of 620–980 cm^{-1}. This variation of the total radiative flux is due to the downward going flux, while the upward going flux varies insignificantly in all spectral regions.

This change of the temperature dependence of the continuum absorption, as in the case with the cooling rates, manifests itself in localization of the maximum response at different altitudes depending on the spectral region (Fig. 6). In the region of 540–620 cm^{-1} the maximum variation of the downward flux resulting from the change of the temperature dependence takes place at the altitude about 700 mbar, whereas the maxima in other spectral regions are closer to the surface.

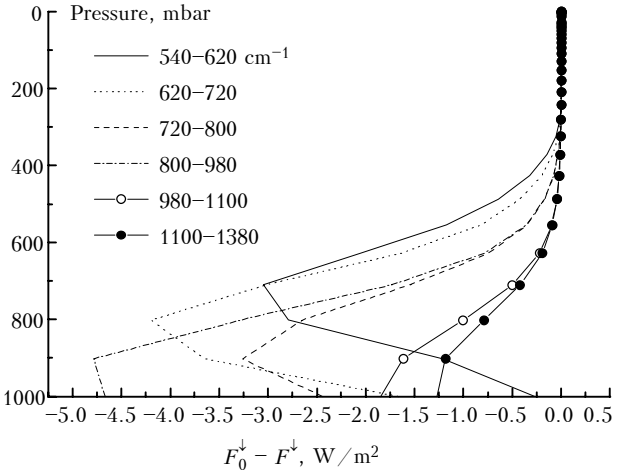

Fig. 6. Differences in the downward going fluxes corresponding to the cases of (H_2O + continuum) and (H_2O + continuum (1800→4000)).

2.2. Influence of the change in the water vapor amount

The proportional change of the water vapor amount at all altitudes (increase or decrease by 25%) manifests itself in localization of the maximum response in the differences of cooling rates at different altitudes depending on the spectral region (Fig. 7).

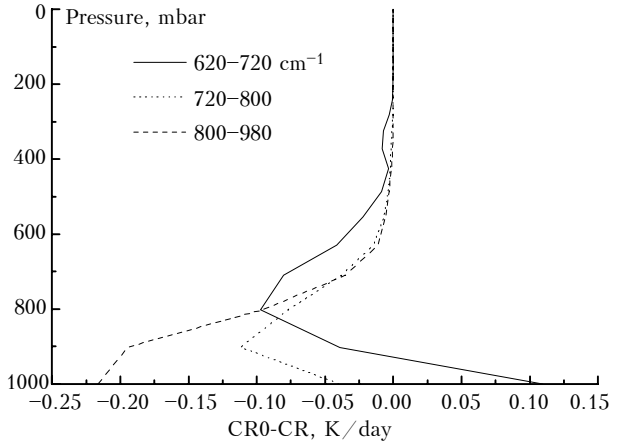

Fig. 7. Differences in the cooling rates corresponding to the cases (H_2O + continuum) and (H_2O + continuum) ($1.25\rho_{H_2O}$) vs. pressure for the spectral regions, where they have the largest values.

As to the relative part of the inclusion of the continuum and proportional change of concentrations,

the former is far more significant than the latter. Besides, the change in concentrations has larger effect on the total cooling rate in the presence of the continuum than in its absence.

As in the case of allowance for the continuum, the upward going flux varies only slightly and monotonically in response to the increasing concentration of water vapor, and the changes in the total flux repeat the changes in the downward going flux. The proportional change of the water vapor amount at all altitudes (increase or decrease by 25%) causes the response in differences in the downward going fluxes at a certain altitude for the first two spectral regions, and the altitude of the maximum response decreases with increasing frequency (Fig. 8). In the other spectral regions the maximum response is localized on the surface.

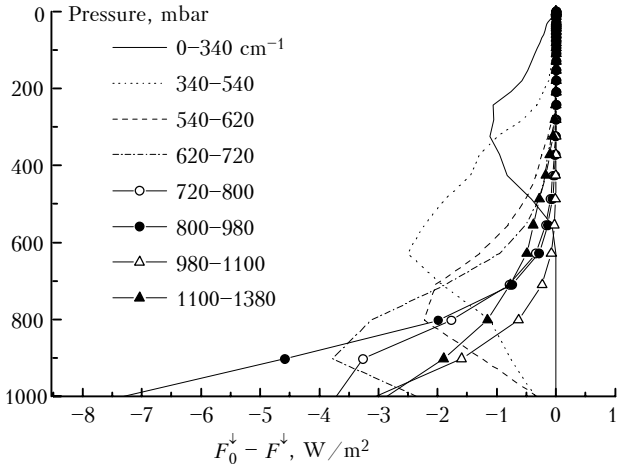

Fig. 8. Differences in the downward going fluxes corresponding to the cases of (H_2O + continuum) and (H_2O + continuum) ($1.25\rho_{H_2O}$).

Thus, it was found that as the water vapor concentration changes at all altitudes, the changes in the cooling rate are localized at some altitude and in some spectral region, and the place of their localization does not coincide with the largest values of these rates themselves. The next problem is to reveal whether or not such selective responses can arise as the H_2O concentration changes in only some altitude regions. Our next attempt is to decrease the water vapor amount at altitudes above ~2 km (starting from the 4th layer) by 5%, while keeping the surface concentration unchanged.

The results are shown in Fig. 9 for the differences in the downward going fluxes and in Fig. 10 for the ordinary and relative differences in the cooling rates. Well-localized maxima in the relative differences of the cooling rates are observed at low pressure. However, they should be treated with care, because the cooling rates at these altitudes are very small, and therefore large errors may occur in the determination of their changes.

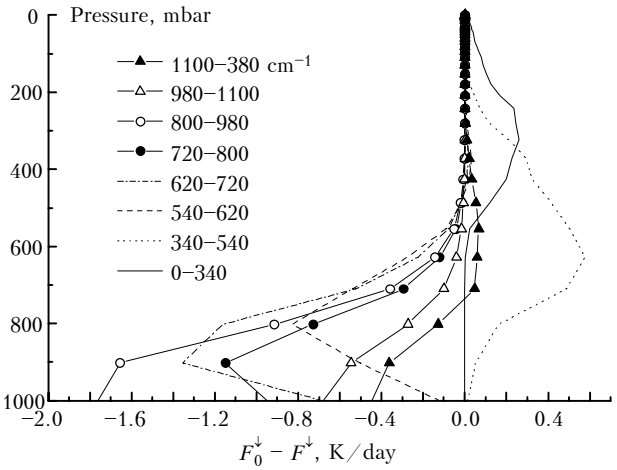

Fig. 9. Differences in the downward going fluxes corresponding to the cases of (H_2O + continuum) and (H_2O + continuum) ($0.95\rho_{H_2O}$ starting from the 4th layer).

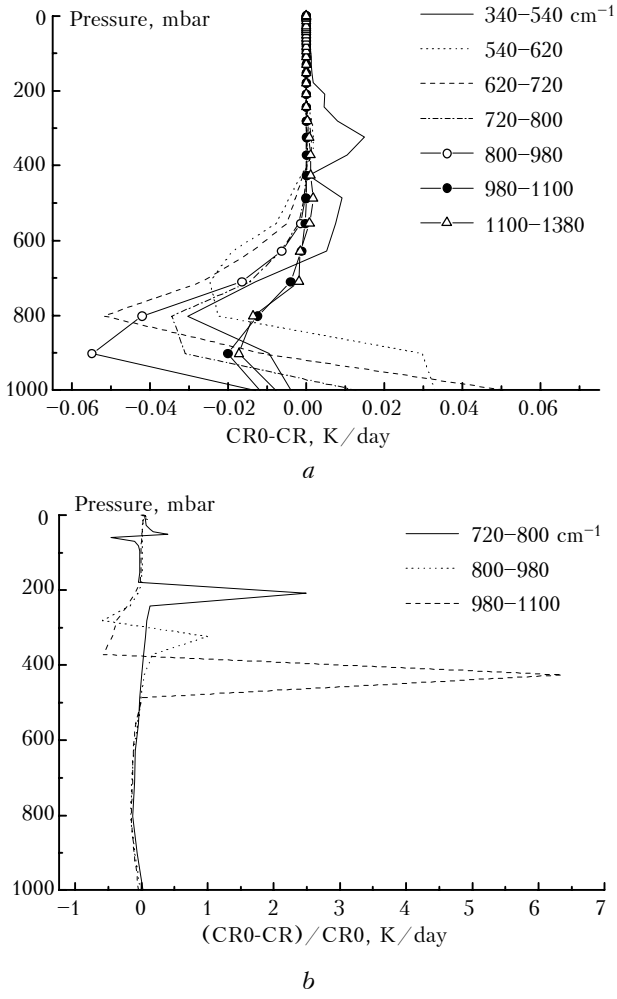

Fig. 10. Ordinary (*a*) and relative (*b*) differences in the cooling rates corresponding to the cases of (H_2O + continuum) and (H_2O + continuum) ($0.95\rho_{H_2O}$ starting from the 4th layer) vs. pressure for the spectral regions, where they have the largest values.

2.3. Allowance for absorption by CO_2

The absorption by CO_2 was taken into consideration in the 540–800-cm^{-1} spectral region, as in Ref. 8. As seen from Fig. 11 the allowance for absorption by CO_2 influences both the upward and downward going fluxes. The upward going fluxes change more markedly at high altitudes starting from ~400 mbar, whereas the downward fluxes experience maximum changes at ~700–500 mbar.

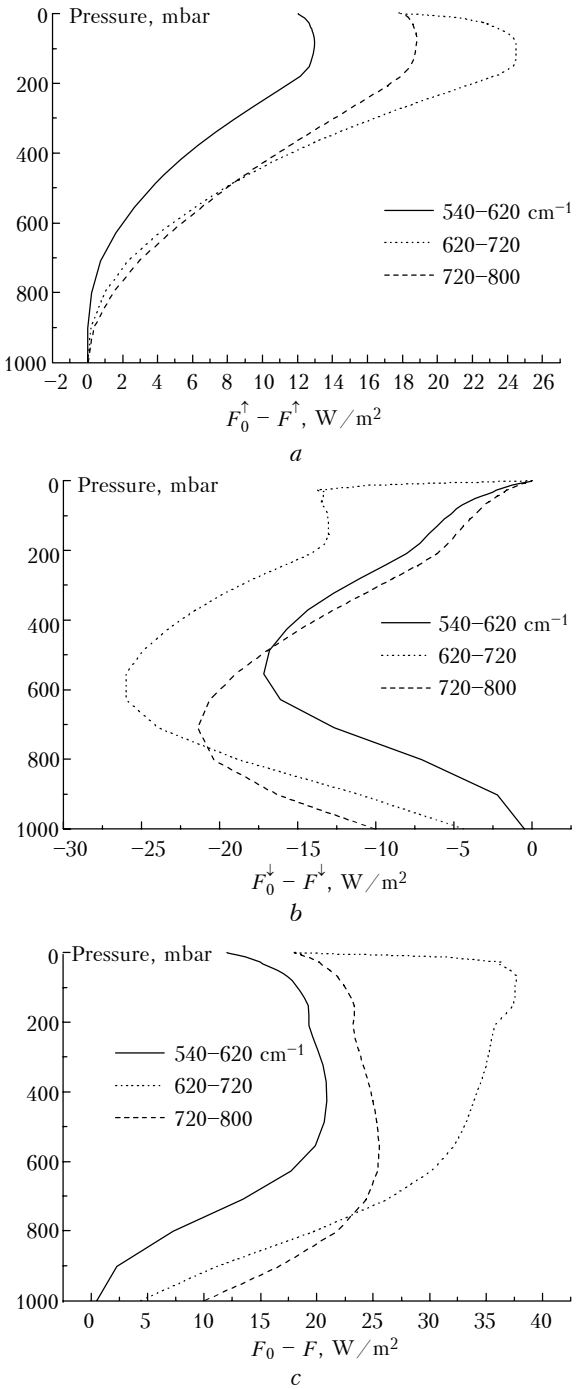

Fig. 11. Differences in the upward going (*a*), downward going (*b*), and total (*c*) fluxes corresponding to the cases of (H_2O + continuum) and (H_2O + continuum + CO_2($3.55 \cdot 10^{-4}$)).

Doubling of the CO_2 concentration leads to similar changes in the fluxes (Fig. 12), except for the 620–720-cm^{-1} region, where the doubling of the CO_2 concentration has practically no effect on the fluxes.

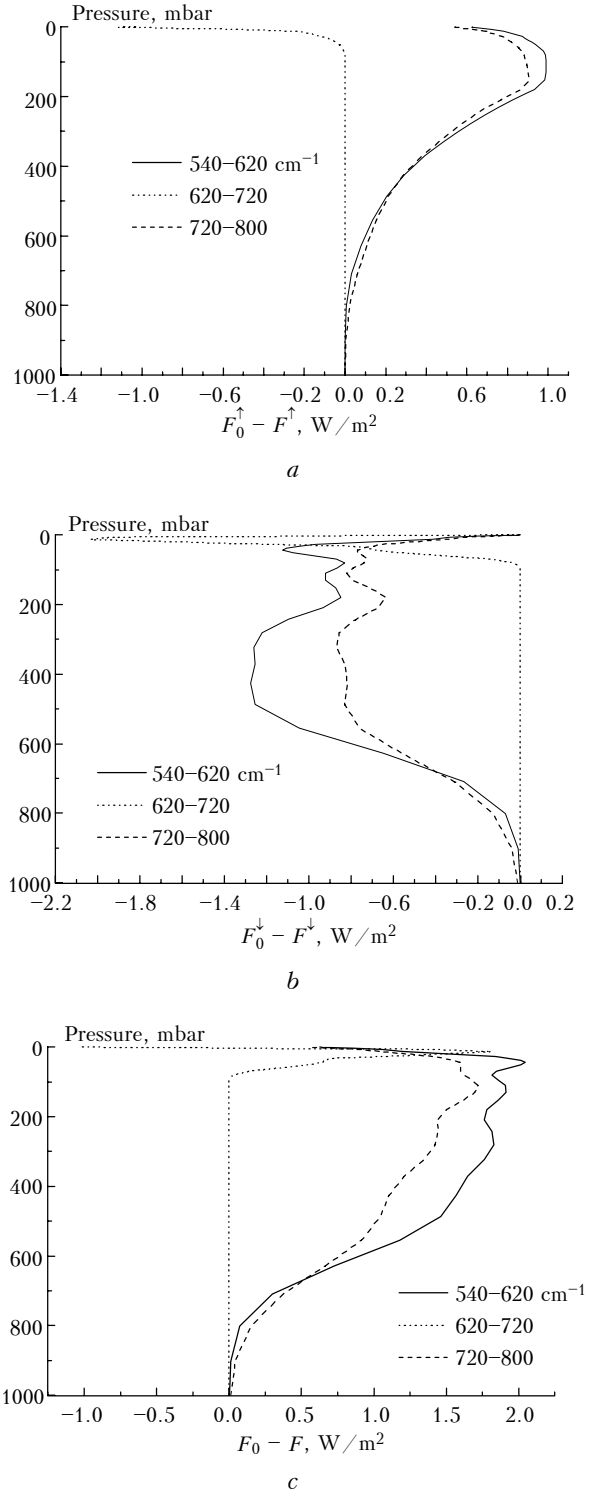

Fig. 12. Differences in the upward going (*a*), downward going (*b*), and total (*c*) fluxes corresponding to the cases of (H_2O + continuum + CO_2 ($3.55 \cdot 10^{-4}$)) and (H_2O + continuum + CO_2 ($7.0 \cdot 10^{-4}$)).

Large localized responses are observed in the relative changes of the cooling rates (Fig. 13). However they are largest at high altitudes and therefore require a closer consideration. A small blurred maximum is observed at the pressure about 700 mbar.

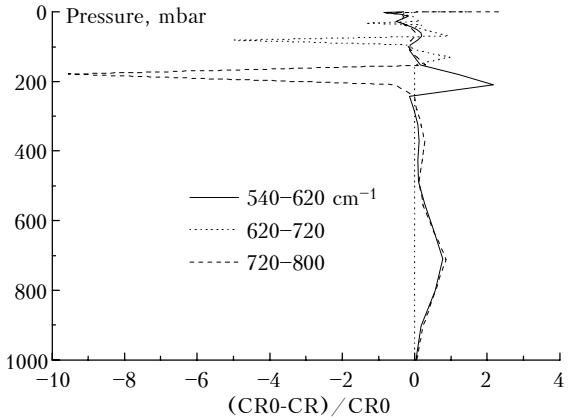

Fig. 13. Relative differences in the cooling rates corresponding to the cases of (H_2O + continuum + CO_2 ($3.55 \cdot 10^{-4}$)) and (H_2O + continuum + CO_2 ($7.0 \cdot 10^{-4}$)).

3. Conclusions

Our calculated results indicate that the cooling rates and radiative fluxes response to changes in concentration of absorbing substances selectively with the altitude and spectral region. A certain type of variations of the absorber amounts results in characteristic changes in the fluxes or rates. Thus, the change in the temperature dependence of the continuum absorption results in the change of the cooling rate in the 620–980-cm^{-1} spectral region at the altitude about 800–900 mbar and in the largest change of the relative cooling rate in the 980–1100 cm^{-1} spectral region at the altitude about 400 mbar. As the water vapor amount increases at all altitudes, the cooling rate in the 800–980-cm^{-1} spectral region increases most strongly on the ground, whereas the maximum decrease of the absorption in the 620–720-cm^{-1} spectral region falls into the altitude region about 800 mbar. If the water vapor amount is changed only above 4 km, the maximum variation of the relative rate falls on 400 mbar level and corresponds to the 980–1100-cm^{-1} spectral region. The changes in the CO_2 concentration can be judged from the change in the relative cooling rate at the level of 200 mbar in the 720–800-cm^{-1} spectral region. As was already mentioned, the qualitative conclusions drawn for this altitude should be treated with care. Nevertheless, detection of changes by the localized responses in the rates or fluxes seems interesting and requires further investigations.

Thus, if it is possible to directly measure the cooling rates, then the global change of the concentrations could be judged from their behavior in certain altitude and spectral ranges. The change of the fluxes also presents some grounds for such judgments, as seen from the above figures.

Our plan for further investigations is to consider more closely the concentration variations in preset altitude layers in order to find evidences in support of or against a selective character of the response of radiative fluxes and cooling rates to these variations. We hope that this will allow us to reveal critical values of variations, which can be then used in investigations into the qualitative changes in the altitude behavior of the atmospheric temperature.

Acknowledgments

The financial support from the Russian Foundation for Basic Research, Grant No. 97–05–65985, is acknowledged.

References

1. E.M. Feigelson, B.A. Fomin, I.A. Gorchakova, et al., J. Geophys. Res. **96**, No. D5, 8985–9001 (1991).
2. B.A. Fomin and J.V. Gershanov, "*Table of the benchmark calculations of atmospheric fluxes for the JCRCCM test cases. Part. I. Long-wave clear sky results*,B Preprint IAE – 5981/1, Moscow (1996), 52 pp.
3. B.A. Fomin and J.V. Gershanov, "*Table of the benchmark calculations of atmospheric fluxes for the JCRCCM test cases. Part II. Short-wave results*,B Preprint IAE – 5990/1, Moscow (1996), 42 pp.
4. S.A. Clough, M.J. Jacono, and J.-L. Moncet, J. Geophys. Res. **97**, 15761–15785 (1992).
5. S.A. Clough and M.J. Jacono, J. Geophys. Res. **100**, 16519–16535 (1995).
6. F. Baer, N. Arsky, J.J. Charney, and R.G. Ellingson, J. Geophys. Res. **101**, No. D21, 26589–26603 (1996).
7. H.E. Brindley and J.E. Harries, J. Quant. Spectrosc. Radiat. Transfer **60**, No. 2, 151–180 (1998).
8. M.-D. Chou, W.L. Ridgway, and M. M.-H. Yan, J. Atmos. Sci. **50**, No. 14, 2294–2303 (1993).
9. R.A. McClatchey, R.W. Fenn, J.E.A. Selby, F.E. Volz, and J.S. Garing, "*Optical properties of the atmosphere*,B Rep. AFCRL–71–0279 (Air Force Cambridge Res. Lab., Bedford, Mass., 1971), 85 pp.
10. R.G. Ellingson, J. Ellis, and S. Fels, J. Geophys. Res. **96**, No. D5, 8929–8953 (1991).
11. S.A. Clough, M.J. Jacono, and J.-L. Moncet, in: *Proc. of the 14th Annual Review Conference of Atmospheric Transmission Models*, 11–12 June 1991, PL–TR–92–2059 Special Reports, No. 267, ed. by L.W. Abreu and F.X. Kneizys (Massachusetts, 01731–5000, 1992), pp. 250–262.